

## Reply for review comments

We sincerely thank you for the efforts you have made to improve our submission to *Natural Hazards and Earth System Sciences*. We have responded to all review comments and have made appropriate modifications to our manuscript related to these comments as detailed in the following paragraphs. The blue-highlighted sentences are the review comments; sentences in black represent our responses to these review comments.

The authors present a study that link the debris flow types to the morphological characteristics of the initiation zone and the entrainment and deposition processes to the debris flow types. The writer identified the following deficiencies:

1) The text, in some parts, is not fluid but hard to read. It looks like an ensemble of pieces more and less linked each other.

We have checked entire manuscript again, and revised sections, which are not linked each other (e.g., explanation about the static model from pg. 4 line 8 to pg. 5 line 20). In addition, we have made a substantial revision in section 6.2, because the scope of the discussion was not clear in the previous version of the manuscript.

2) Authors through a static equilibrium-based relationship (equation 5), obtain angles corresponding to different debris flow types or the sediment concentration of debris flow corresponding to bed slope angles, if the other quantities are known. If used for dynamic computation (i.e. the sediment volume concentration of the flowing material) this equation is misleading. In the case of motion, the equation (5) is a bit different (Lanzoni et al., 2017) and is obtained through the ratio between the basal bed shear stress and the basal normal stress. Moreover in the case of flowing material, the angle  $\phi$  is not the static friction angle but the quasi-static of dynamic friction angle (Lanzoni et al., 2017). Therefore, also the sentence “Thus, not only.....Eq(5)”, is uncorrected. Therefore, I suggest the authors to write that an equation of the same structure of eq. (5) can be obtained through the ratio between the basal bed shear stress and the basal normal stress that have a similar structure to the ration between shear stress and strength (Lanzoni et al., 2017).

Some governing equations for the debris flow in previous studies explained that only static frictional force (coulomb force), which can be obtained by the volume concentration of the flowing material, acts on the surface of the erosible bed (e.g., Egashira et al., 2001; Takahashi, 2014). However, as the reviewer pointed out, other studies consider flow dynamics differently. In any of these cases, we think the ratio between the shear stress and the normal stress at river bed is an important factor controlling flow characteristics. We have added the sentence suggested by the reviewer (pg. 4, lines 23-25). The sentence in p. 4 line 22-23 intended to mention that other types of sediment transport processes also satisfy the Eq. (5). We have revised the sentence to clarify what we mean (pg. 4, lines 26-27).

3) About triggering of debris flow, both the experiments of Gregoretti (2000) and the theoretical computations of Gregoretti (2008) clearly show that the entrainment of debris material into a water stream is provided by the surficial erosion of the debris layer rather than by the slide of the debris layer. Moreover, field works of Berti and Simoni (2005) , Cannon et al. (2008), Coe et al. (2008), Gregoretti and Dalla Fontana (2008), Theule et al. (2012), Hurliman et al. (2014), Degetto et al. (2015), Hu et al. (2016) point to a triggering mechanism where runoff erode the sediments and spread them along flow depth rather than the slide of a saturated mass. Recent works of Gregoretti et al. (2016) and Rengers et al. (2016) show that runoff descending from cliffs is an impulsive phenomenon characterized by a peaked hydrograph and that the impact of peak against debris deposits entrain enough material to have a solid-liquid current. Finally, authors cited the work of Kean et al. (2013) and Navratil et al. (2013). In the first work, it is expressly written that debris flow initiation by surface runoff is different from the debris flow initiation by shallow landslide (the title of the work deals with runoff-generated debris flow), while in the second it is stated that debris flow is initiated by surface runoff rather than landslide. Therefore, if the authors intend to use their slide model, they should state that channelized debris flow initiate by runoff as a surficial erosion (cite the references above) and that they approximate it by a “slide” model using the calculation that Prancevic et al. (2014) show.

Many debris flows in the Ohya landslide were also initiated by the erosion of the debris material by the surface runoff (Imaizumi et al., 2016). As the reviewer points out, erosion by the surface runoff is the predominant initiation mechanism of the debris flow. In the Ohya landslide, sliding of the debris material was also monitored. Our monitoring site is possibly in the traditional slope gradient range from fluvial processes to the failure of the debris deposits when we consider initiation mechanism of the debris flow like Prancevic et al. (2014). As the review suggested, we have added statements that many debris flows in the Ohya landslide and other debris flow torrents were triggered by the surface erosion. In addition, we noted that relationships between topography and type of sediment transport were discussed by approximation of the sediment transport type by the simple static models (pg. 5, lines 13-20).

Imaizumi, F., Tsuchiya, S. & Ohsaka, O. (2016) Field observations of debris-flow initiation processes on sediment deposits

in a previous deep-seated landslide site, *Journal of Mountain science*, 13: 213. doi:10.1007/s11629-015-3345-9

About 6.1, the writer agrees with authors that sediment availability determines the type of debris flows but has some concern about partially saturated debris flow even if stated by other authors (e.g. Iverson and Vallance, 2001). They could be very dense debris flows, where fluid phase is just under the surficial sediments. Measurements carried out at Illgraben (McArdell et al., 2007) show a flow density of the front that approximates that of a saturated terrain. An alternative way is that of very dense debris flow rich of debris material and more fluid debris flow. About the outcome of the correspondence between short-lasting rainfall and partially saturated debris flows and that between long-lasting rainfalls and saturated debris flows, the field experiences in the initiation area Cancia debris flow given by Bernard et al. (2016) and Gregoretti et al. (2016) seem to contradict it. At Rovina di Cancia (Northeastern Italian Alps) an hyperconcentrated flow occurred about 11 days later a partially saturated debris flows (according to the author definition; see the video at the following link <https://www.youtube.com/watch?v=oKQSZVwOuRo>). The rainfall depths were just a bit smaller in the second event even if the terrain was not dry as for the first event (Gregoretti et al., 2016). The main reason is that after the first event, channel did not recharge and the quantity of entrained sediments in the second event in the initiation reach was at least an order smaller than that entrained during the first event.

Thank you for telling us an interesting video in YouTube. As the reviewer comments, density of debris flow can be very high (close to that of saturated terrain) particularly at the head of surges even in the gentler channel (McArdell et al., 2007; McCoy et al., 2010; Okano et al., 2012). Unfortunately, we do not have data related to the internal structure of the debris flow (e.g., thickness of the unsaturated layer, depth profiles of solid concentration and flow velocity). Thus, we cannot deeply discuss dynamic mechanism of the flow. We have revised statements on the partly saturated debris flow in section 6.1 to clarify relationship between results in our study and previous studies (pg.20, lines 11-18). We have also discussed limitation in our analyses in the end of discussion (pg. 22, lines 21-27). As presented in Takahashi (2007) and Lanzoni et al. (2017), we think depth profile of the dynamic force affected by the slope gradient and the particle size relative to the flow depth should be considered to complete explanation of the dense debris flows. On the other hand, our simple static-force analyses and results of the field monitoring implied that unsaturated sediment transport frequently occur in the steep terrains. We think that point is worth to be emphasized in this paper.

We checked Gregoretti et al. (2016, WRR) but could not find statements on the flow characteristics and rainfall pattern triggering debris flow. However, we agree with the reviewer's comment that recharge of the sediments into valley bottom affect volume of the sediment entrained by debris flows. Our monitoring results also implies that volume of debris flow material affects flow characteristics (Fig. 6). In the end of the section 6.1, we have emphasized importance of the amount of the debris flow material and that of water supplied on the debris flow type (pg. 21, lines 10-14). Grain size, amount of debris flow material, and topography may affect difference in the flow characteristics and initiation mechanisms among debris flow torrents. In the end of the paper (in conclusion), we have added statements that we need to collect data in other debris flow torrents with different site conditions (e.g., grain size, slope gradient) for the further understanding of interactions between the debris flow characteristics and the topography (pg. 23, lines 20-24).

1. Page 1 – line 20: the sentence “The small-scale channel gradient....” is unclear.

We have revised the sentence. Statements on characteristics of channel morphology (slope gradient) were added (pg. 1, lines 23-25).

2. Page 1 - line 26: has been

We have replaced “have” to “has” (pg. 1, line 28).

3. Page 1 - line 28: the word “activities” after “monitoring” is missing.

As suggested by the reviewer, we have added “activities” (pg. 2, line 1).

4. Page 2 - line 1: some parts of the sentence “Understanding .....system” are unclear.

We have revised the sentence. Now the sentence is “factors affecting debris-flow characteristics in the initiation zone (e.g., temporal changes in the solid fraction) is still unclear” (pg. 2, lines 3-4).

5. Page 2 – line 4: perhaps the reference Takahashi 2007 is better than Takahashi 1991.

We have replaced the reference “Takahashi, 1991” to “Takahashi, 2007” (pg. 2, line 6).

6. Page 2 - line 18: add the reference Gregoretti and Dalla Fontana (2008).

We have added the reference Gregoretti and Dalla Fontana (2008) (pg. 2, line 23).

7. Page 4 – line 5: what does it mean “is the exception ..... between  $\alpha$  and  $\phi$ ?”.

We have revised the explanation about pyroclastic flow. The relationship between  $\alpha$  and  $\phi$  expressed as Eq. (4) cannot be applicable to the pyroclastic flow (pg. 4, lines 8-13).

8. Page 4 – line 30: the sentence “The explanations.....2014)” is unclear as it regards the terrain formed by the sediment mass:

what does it means? Moreover, the relationship given by Takahashi (2014) should be written.

The sentence explained relationship between solid fraction and channel gradient. In order to clarify the relationship between solid fraction and channel gradient, we have added Eq. (6). In addition, we replaced “terrain” to the “channel gradient” (pg. 5, lines 5-6).

9. Page 6 – lines 9-11: the sentence “Most of the channel....low” is bad written and misleading.

This sentence explains the channel bed condition in the monitoring site. We have improved the sentence (pg. 7 line 2-4).

10. Page 7 – line 8: P2 is not in fig. 2a but in fig. 2b

We have removed “a” after “Fig. 2” (pg. 8, line 7).

11. Page 8 – lines 2 and 6: perhaps mean flow depth velocity or flow depth averaged velocity should be better than “mean velocity of all layers of the flow”.

We have replaced “mean velocity of all layers of the flow” to “flow depth averaged velocity” (pg. 8, line 14).

12. Page 9 – line 14: the sentence “The location of ...” is bad written.

We have revised the sentence. Now the sentence is “The location of this scan position varied with time because it was in the valley bottom where the topography changed due to erosion and deposition by debris flows.”(pg. 10, lines 4-5).

13. Page 11 – line 5 and following: which technique did used the authors to obtain the map of storage through the photographs taken at P1 and P4?

We have added detailed explanation about the estimation method of the storage (pg. 11, line 14 - pg. 12, line 1).

14. Page 12 – line 3: substitute “section between sites” with “reach between the sites”.

We have replaced “section between sites” to “reach between the sites” (pg. 12, line 7).

15. Page 12 – line 9: “high value of total rainfall depth” instead of “high total rainfall”

We have replaced “high total rainfall” to “high value of total rainfall depth” (pg. 12, line 13).

16. Page 12 – line 10: “characterized by high intensity” instead of “of high intensity”

We have replaced “of high intensity” to “characterized by high intensity” (pg. 12, line 14).

17. Page 12 – line 14: “varied between the events” instead of “differed between events”.

We have replaced “differed between events” to “varied between the events” (pg. 12, line 18).

18. Page 12 – lines 14-16: the sentence “For example.....(Fig. 5)” should be rewritten as: For example in the event of 5 August 2008, 88% of debris flow surges (percentage respect to the total event duration) was composed of partly saturated flow, while in the event of 30 August 2004 (Fig. 5), 90% in time of the phenomenon was composed of fully saturated flow.

We have rewritten the sentence as suggested by the reviewer (pg. 12, lines 18-20).

19. Page 12 – lines (16-19): sentence bad written: what does it mean the relation between camera location and debris flow characteristics?

Originally we meant that difference in the channel gradient among camera locations potentially affects difference in the flow type. However, the channel gradient changes with time even at the same camera location. Therefore, now we think first half of the sentence was not needed (pg. 12, line 20).

20. Page 12 – lines (19-24): sentences very bad written; please rewrite them stating that the typology of rainfall determined the flow typology.

We have rewritten the sentence. We think the sentence is easy to read now (pg.12, lines 22-25).

21. Page 14- lines (8-9): the writer does not understand the sentence “The roughness of the ground surface attributable to boulders.....” How the roughness that is a length can be estimated by a slope gradient map? Moreover, the authors should introduce the definition of slope gradient or explain it.

We think the term ”roughness” was not appropriate. We have revised the sentence. We also explained how the slope gradient was calculated (pg. 14, line 8-10).

22. Page 14 – line 13: authors should specify that obtained the DEM after using TLS data and the method they used for determining the slope gradient.

We have added explanations how to obtained DEMs from the TLS point clouds (pg. 10, line 19-21). We have also presented calculation method of the slope gradient (pg. 14, lines 8-9). We used the method proposed by Horn (1981).

23. Page 14 – line 14: please place “the” before highest

We have added “the” in front of the “highest” (pg. 14, line 15).

24. Page 14 – line 17: talus slope is the slope gradient?

We have rephrased the sentence. Now the phrase is “a histogram of the slope gradient in talus slopes...” (pg. 14, line 18).

25. Page 15 – caption of Figure 7: calculated after using TLS data.....

We have revised the figure caption as suggested by the reviewer (pg. 15)

26. Page 16 – lines (1-8): the writer does not understand what the authors mean. In other words, what does it the meaning of the channel topography forming after debris flow occurrence?. It means that all the channel was flooded by debris flow or that the debris flow changed the bed.

We have added explanation about the aim of analyses on the longitudinal channel topography (pg. 16, lines 2-4). We tried to find out relationships between the flow type and the longitudinal profile of the channel (channel gradient) formed by the debris flow in the steep debris-flow initiation zone. Most part of the channel topography in the section between points A and E was changed by the debris flows on 30 September 2012 and 6 August 2015. In contrast, channel topography was not largely changed by the small debris flow on 17 August 2015. Therefore, we assumed that the channel profile on 23 August 2015 reflected characteristics of the debris flow on 6 August 2015, rather than that on 17 August 2015 (pg. 16, lines 9-10).

27. Page 16 – lines (9-14): even in these sentences the writer does not understand what the authors mean. Visual inspection of the two bed profiles of Figure 9a (are they from post-event surveys?) show that there is an high lowering of the bed profiles at the beginning and ending reaches. Authors should provide a much better description/comment of this figure.

We intended to explain similar characteristics as the reviewer comments. We have rewritten the paragraph (pg. 16, lines 11-18). The topography was obtained by the post-event surveys (pg. 16, line 2).

28. Page 17 – caption of Figure 9: authors should specify that the profiles correspond to post-event surveys.

We have added timing of the debris flow events in the figure caption (pg. 17). Thus, now it is clear that the profile was measured after the debris flow events.

29. Pages 19-20. All the comments about  $\alpha_1$ ,  $\alpha_2$  the storage volume and slope gradient should consider that the middle part of the channel was not interested by erosion phenomena. Therefore, the authors should explain a reason and then exclude it from the further comments. Moreover, the sentence between pages 19 and 20 is not clear.

We have discussed the reason why the channel bed deformation was not clear in the middle part of the profile (pg. 16, line 33-pg. 17, line 2). Channel was narrowed because of the massive rock cliffs at the left bank. Therefore, flow depth in this section may exceeds that in the other sections. High stream power attributed to the high flow depth may restricted deposition of the sediments, possibly resulting in the small channel bed deformation. We also excluded a sentence about inactive section (pg. 20, line 2). We revised the sentence which, was between pages 19 and 20 (pg. 19, line 14-pg. 20, line 2).

30. Page 21 - lines 14-15. The explanation on the effect of grid size on hystogram shape should be coupled with some estimation of roughness (i.e. median grain size or something else) . Moreover, the authors should initiate the subsection explaining the reasons they produced the histograms.

We have added discussion between the shape of the histograms and grain size (pg. 21, lines 20-25). We think that the influence of the grain size on the slope gradient should be eliminated when we discuss relationship between the slope gradient and the sediment transport type (pg. 21, lines 25-28). Analyses of the histogram provides us idea on the influence of roughness attributed to the grain size on the slope gradient. We have added explanation about importance such analyses in the top of the section (pg. 21, lines 16-20).

31. Pages 21-22: the writer does not understand well the scope of the written sentences: authors should clearly rewrite them. For instance, fully saturated debris flow removed only fine sediments while partially saturated debris flows washed out entire bottom reaches. The writer thinks that the amount of entrained material depend also on the main characteristics of the of the solid-liquid current: flow depth, sediment concentration and velocity that in the case of coarse grained debris flow depends also on the runoff discharge (Lanzoni et al., 2017).

We agree with the reviewer’s comment that the amount of entrained material depends on the flow depth, sediment concentration and velocity (this can be expressed as a function of flow depth and sediment concentration). In this section, we did not discuss amount of entrained material, but we discussed relationship between the (channel) topography and the type of the sediment transport. In order to make the topic clear, we have changed title of the section to “Influence of the sediment transport type on the slope gradient of terrains”. The topic about the selective transport of the channel deposits would be not necessary in this paper. In addition, that topic may have obscured scope of the discussion. Therefore, we have removed the statements on the selective transport. We also revised the end of the section to emphasize importance of the relationships between the channel topography and type of sediment transport (pg. 22, lines 28-29).

# Interactions between the accumulation of sediment storage and debris flow characteristics in a debris-flow initiation zone, Ohya landslide body, Japan

Fumitoshi Imaizumi<sup>1</sup>, Yuichi S. Hayakawa<sup>2</sup>, Norifumi Hotta<sup>3</sup>, Haruka Tsunetaka<sup>4</sup>, Okihiko Ohsaka<sup>1</sup>,  
5 Satoshi Tsuchiya<sup>1</sup>

<sup>1</sup>Faculty of Agriculture, Shizuoka University, Shizuoka, 422-8529, Japan

<sup>2</sup>Centre for Spatial Information Science, The University of Tokyo, Kashiwa, 277-0871, Japan

<sup>3</sup>Faculty of Life and Environmental sciences, University of Tsukuba, Tsukuba, 305-8572, Japan

<sup>4</sup>Graduate School of Life and Environmental sciences, University of Tsukuba, Tsukuba, 305-8572, Japan

10 *Correspondence to:* Fumitoshi Imaizumi (imaizumi@shizuoka.ac.jp)

**Abstract.** Debris flows often occur in steep mountain channels, and can be extremely hazardous as a result of their destructive power, long travel distance, and high velocity. However, their characteristics in the initiation zones, which could possibly be affected by temporal changes in the channel topography associated with sediment supply from hillslopes and the evacuation  
15 of sediment by debris flows, are poorly understood. Thus, we studied the interaction between the flow characteristics and the topography in an initiation zone of debris flow at the Ohya landslide body in Japan using a variety of methods, including a physical analysis, a periodical terrestrial laser scanning (TLS) survey, and field monitoring. Our study clarified that both partly and fully saturated debris flows are important hydrogeomorphic processes in the initiation zones of debris flow because of the steep terrain. The predominant type of flow varied temporally and was affected by the volume of storage and rainfall patterns.  
20 The small-scale channel gradient (on the order of meters) formed by debris flows differed between the predominant flow types during debris flow events. The relationship between flow type and the slope gradient could be explained by a simple analysis of the static force at the bottom of the sediment mass. Partly saturated debris flow formed channel topographies with a theoretical channel gradient for the partly saturated flow (22.2 – 37.3° in the Ohya landslide), while fully saturated debris flow formed channel topographies with gentler channel gradient (<22.2° in the Ohya landslide).

## 25 1 Introduction

Debris flows often occur in steep mountain channels and can be extremely hazardous as a result of their destructive power, long travel distance, and high velocity (Lin et al., 2002; Cui et al., 2011). To lower the hazard of debris flow, field monitoring has been conducted in many torrents in the world including Switzerland (McArdell et al., 2007; Berger et al., 2011b), Italy (Arattano, 1999; March et al., 2002; Arattano et al., 2012), the United States (McCoy et al., 2010; Kean et al., 2013), and China

(Zhang, 1993; Hu et al., 2011). Many of these monitoring activities have been undertaken in the transportation zones of the debris flows, with only a few observations undertaken in their initiation zones, where the unstable sediment start to move (Berti et al., 1999; McCoy et al., 2012; Kean et al., 2013). Thus, factors affecting debris-flow characteristics in the initiation zone (e.g., temporal changes in the solid fraction) is still unclear.

5 Debris flows can be classified into various types according to their flow dynamics, solid fractions, and material types (Coussot and Meunier, 1996; Hunger, 2005; Takahashi, 2007). Multiple flows types appear even in the same torrent (Imaizumi et al., 2005; Okano et al., 2012). However, in situ classification of debris flow type is mainly based on monitoring results obtained in the transportation zone. Field monitoring conducted at multiple sites along a debris flow torrent have revealed that flow characteristics (e.g., solid fraction and boulder size) and discharge change as the flow migrates downstream and is affected  
10 by erosion and deposition (Takahashi, 1991, Berger et al., 2011b; Arattano et al., 2012). Thus, flow characteristics in the transportation zone possibly differ from those in the initiation zone. In the initiation zone, flows containing an unsaturated layer have also been observed during field monitoring (Imaizumi et al., 2005; McArdell et al., 2007; Imaizumi et al., 2016b). Such information is needed to explain the sequence of debris flow processes from initiation in the headwaters to termination at the debris flow fan.

15 The topography along debris flow torrents reflects the characteristics of a debris flow event (Whipple and Dunne, 1992; Coussot and Meunier, 1996; Imaizumi et al., 2016a). The curvature of the terrain can be used to determine the relationship between shear stress and shear strength (Staley et al., 2006). Many observations of the relationships between topography and flow characteristics have been made in the lower part of the debris flow torrents, while such findings are limited in the debris-flow initiation zone. In many cases, the channel gradient in the initiation zone is greater than 20° (VanDine 1985; Pareschi et al. 2002; McCoy et al., 2013; Hürlimann et al., 2015). In terms of debris flows caused by the transportation of loose sediment on the floor of a valley, both the volume and grain size of debris flow material (e.g., channel deposits and talus slope) change over time in association with the sediment supply from hillslopes, as well as the evacuation of sediment by debris flows and fluvial processes (Bovis and Jakob, 1999; Imaizumi et al., 2006; Gregoretti and Dalla Fontana, 2008; Berger et al., 2011a).  
20 Although some previous studies have investigated the relationship between characteristics of the debris flow material and initiation condition of a debris flow (Bovis and Jakob, 1999; Jakob et al., 2005; Schlunegger et al., 2009; Chen et al., 2012), only a few have considered the relationship between flow material and flow characteristics (Kean et al., 2013; Imaizumi et al., 2016b). The difficulty in monitoring debris flows in steep and dangerous initiation zones has prevented the collection of the field data needed to clarify the relationship between flow characteristics and flow material.

In the debris-flow initiation zone at the Ichinosawa catchment within the Ohya landslide, Japan, field monitoring has been  
30 undertaken since 1998 (Imaizumi et al., 2005; Imaizumi et al., 2006). This site is suitable for monitoring because of the high debris-flow frequency (about three or four events per year) that occur due to the mobilization of storage (i.e., talus cone and channel deposits) around the channel. In addition, detailed topographic measurements by terrestrial laser scanning (TLS) have been undertaken periodically since 2011 (Hayakawa et al., 2016).

In this study, we investigated the relationship between the slope gradient and type of sediment transport based on a simple analysis of the static force. Then we considered the relationship between the accumulation conditions of storage (i.e., slope gradient and volume of storage) and debris-flow characteristics based on field monitoring results in the Ohya landslide. Our specific objectives were to explain the relationship between topography and sediment transport type by simple models, clarify temporal changes in the channel topography of the debris-flow initiation zone due to the occurrence of debris flows, and clarify the interaction between the characteristics of sediment storage (i.e., volume and slope gradient) and the debris flow type.

## 2 Slope gradient and type of sediment transport

In this section, we describe our analysis of the balance of static force at the bottom of a sediment mass to assess the relationship between slope gradient and the type of sediment transport. Shear stress at the bottom of a sediment mass needs to exceed shear strength for the sliding of a stable debris mass (Takahashi, 1991; Prancevic et al., 2014; Imaizumi et al., 2016c). Similarly, shear stress needs to exceed shear strength at the bottom of a traveling sediment mass for the continuity of travel (Takahashi, 1991; Watanabe, 1994). Under the assumption that cohesion is negligible, shear stress  $\tau$  and shear strength  $\tau_r$  at the bottom of sediment mass can be given as follows:

$$\tau = \{(1 - \eta_w)[(1 - n)\gamma_s + nS\gamma_w] + \eta_w[(1 - n)\gamma_s + n\gamma_w]\}\sin\alpha, \quad (1)$$

$$\tau_r = \{(1 - \eta_w)[(1 - n)\gamma_s + nS\gamma_w] + \eta_w[(1 - n)(\gamma_s - \gamma_w)]\}\cos\alpha\tan\phi, \quad (2)$$

where  $\eta_w$  is the ratio of the depth of the saturated zone ( $h_w - z_1$ ) to the depth of the sediment mass ( $h - z_1$ ),  $h_w$  is the height of the water table,  $z_1$  and  $h$  are the height at the bottom and surface of the sediment mass, respectively,  $n$  is the porosity of sediment,  $\gamma_s$  is the force of gravity acting on a unit volume of sediment,  $\gamma_w$  is the force of gravity acting on a unit volume of water (or interstitial water for debris flow),  $S$  is the degree of saturation in the unsaturated zone,  $\alpha$  is the slope gradient, and  $\phi$  is the effective internal angle of friction (Fig. 1). Note that  $\alpha$  is the slope gradient of the potential sliding surface when we consider the initial movement of the stable mass, whereas it is the gradient of the surface topography when we consider the migration of the traveling sediment mass. The  $n$  in the moving sediment mass is similar to that of stable sediment when dispersion of the sediment particles is not significant, while  $n$  in the moving sediment mass greatly exceeds that of the stable sediment when the particle dispersion associated with collision among the particles is significant (e.g., fully saturated debris flow). Based on Eqs.(1) and (2), the critical condition for the movement of sediment mass ( $\tau_r = \tau$ ) can be given as follows (Imaizumi et al., 2016c):

$$\frac{\tan\alpha}{\tan\phi} = \frac{(1 - \eta_w)[(1 - n)\gamma_s + nS\gamma_w] + \eta_w[(1 - n)(\gamma_s - \gamma_w)]}{(1 - \eta_w)[(1 - n)\gamma_s + nS\gamma_w] + \eta_w[(1 - n)\gamma_s + n\gamma_w]}. \quad (3)$$

Based on the  $\eta_w$ , three typical sediment transport types were considered: fully unsaturated ( $\eta_w = 0$ ), partly saturated ( $0 < \eta_w < 1$ ), and fully saturated ( $\eta_w = 1$ ). In case of  $\eta_w = 0$ , Eq. (3) is expressed as:

$$\tan\alpha = \tan\phi, \quad (4)$$

If the slope gradient  $\tan\alpha$  exceeds  $\tan\phi$ , the sediment mass can move without any saturation (Fig. 1a). In other words, Eq. (4) expresses the lowest boundary of the slope gradient for the movement of the fully unsaturated sediment mass (hereafter referred to as  $\alpha_1$ ). There are several types of sediment transport in fully unsaturated conditions, such as rockfall, dry granular flow, and dry ravel, which is the gravitational transport of ground surface materials by bouncing, rolling, and sliding (Carson, 1977; Dorren, 2003; Gabet, 2003). Although physical mechanisms between individual particles (i.e., rockfall and dry ravel) and flows of grains (i.e., dry granular flow) are different in terms of the interactions among particles, the slope gradient of talus slopes, which are formed by fully unsaturated sediment transport processes, are usually similar or slightly smaller than  $\phi$  regardless of the transport type (Kirkby and Statham, 1975; Carson, 1977; Mangeney et al., 2007). Field surveys and laboratory experiments showed that pyroclastic flow, which is a fluid composed of a mixture of air and particles, sometimes reaches terrain much smaller than  $\phi$  (Yamashita and Miyamoto, 1993; Takahashi and Tsujimoto, 2000). Thus, the pyroclastic flow does not satisfy Eq. (4). Although the pyroclastic flow is an important sediment transport process in areas with many fine particles (i.e., volcanic areas), we did not consider that in this study because we focused on sediment transport processes in areas in which gravel, cobbles, and boulders dominated the debris flow material.

The relationship between slope gradient and the volumetric sediment concentration ( $1 - n$ ) in a saturated sediment mass is given by substituting 1 into  $\eta_w$  in Eq. (3):

$$\tan\alpha = \frac{(1 - n)(\gamma_s - \gamma_w)}{(1 - n)\gamma_s + n\gamma_w} \tan\phi. \quad (5)$$

Note that  $n$  here becomes larger than the  $n$  of storage when sediment particles start to disperse by collision with other particles. By the transformation of Eq. (5), relationship between the solid concentration in the steady-state flow (called equilibrium concentration) and the slope gradient is obtained (Takahashi, 1991; Egashira et al., 2001, Takahashi, 2014):

$$C = \frac{\gamma_w \tan\alpha}{(\gamma_s - \gamma_w)(\tan\phi - \tan\alpha)}, \quad (6)$$

where  $C$  is the solid fraction ( $C = 1 - n$ ). An equation of the same structure of Eq. (6) can be obtained through the ratio between the basal bed shear stress and the basal normal stress that have a similar structure to the ration between shear stress and strength (Lanzoni et al., 2017). Equation (5) just considers shear strength and shear stress at the bottom of the sediment mass, but does not consider the conditions of the fluid of the sediment mass. Thus, the sliding of the sediment mass without any fluid and the plug flow, of which the upper layer in the sediment mass is not fluid, also satisfies Eq. (5). By substituting the porosity of the storage into  $n$ , Eq. (5) expresses the slope gradient needed for the entrainment of a fully saturated sediment mass, with no dispersion of particles (hereafter referred to as  $\alpha_2$ ). When the slope gradient of the terrain ranges between  $\alpha_1$  and  $\alpha_2$ , the transportation of a partly saturated sediment mass occurs (Fig. 1b) (Watanabe, 1994; Imaizumi et al., 2005; Imaizumi et al., 2016c). Partly saturated sediment transport has also been observed in channels gentler than  $\alpha_2$  (i.e., channel gradient  $< 10^\circ$ ) (McArdell et al., 2007; McCoy et al., 2010; Okano et al., 2012). However, the appearance of partly saturated sediment



transport in such gentler channels is generally limited at the front of a surge. In torrents gentler than  $\alpha_2$ , the existence of surface flow over debris flow material is theoretically required for the initiation of debris flow (Fig. 1c) (Takahashi, 1991; Imaizumi et al., 2016c). Once sediment starts to move, it spreads throughout the flow (Fig. 1d). Thus the volumetric solid concentration is lower than that in sediment storage ( $1 - n$ ).

5 The explanations above (Eqs. (5) and (6)) are also applicable to the relationship between the solid fraction of the debris flow and the channel gradient formed by erosion and deposition during passage of the debris flow (Takahashi, 1991; 2014). If the amount of water in the sediment mass from the upper channel reaches is constant, the slope gradient of the terrain approaches the gradient given by the substitution of  $\eta_w$ ,  $n$ , and  $S$  of the sediment mass into Eq. (3) as a result of deposition and erosion.

10 In this study, we call any partly and fully saturated sediment transport processes as partly and fully saturated debris flows, respectively. Although some sediment transport processes at our monitoring site were not typical debris flows, such as those composed of a mixture of sediment and water (Takahashi, 1991; Coussot and Meunier, 1996), we believe the processes at our study site directly or indirectly contributed to the initiation of debris flow. Field monitoring in many debris flow torrents, including Ohya landslide, showed that debris flows on debris deposits laid on the steep channels usually initiate by runoff as a surficial erosion (e.g., Coe et al., 2008; Gregoretti and Dalla Fontana, 2008; Degetto et al., 2015; Imaizumi et al., 2016b). In  
15 such cases, because sediment transport was affected by the hydrodynamic forces (Gregoretti, 2000; Gregoretti and Dalla Fontana, 2008; Prancevic et al, 2014), solid concentration of the debris flow does not satisfy Eq. (5) at least in the initial stage of the debris flow. In addition, above discussion does not consider dynamic force in the flow. Therefore above models cannot strictly explain all sediment transport processes in the debris flow torrents. In this study, however, we approximated such complex flow conditions by above simple static models as with Takahashi (2014) and Prancevic et al. (2014) in order to figure  
20 out overall interactions between sediment transport type and topography in the debris flow initiation zone.

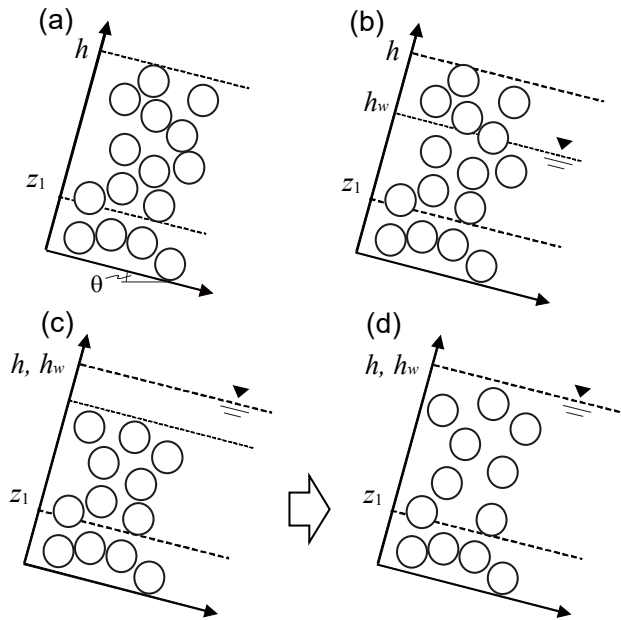


**Figure 1: Schematic diagram of sediment transport types: (a) dry (fully unsaturated), (b) partly saturated, (c) surface flow over sediments, which triggers fully saturated sediment transport, (d) fully saturated sediment transport.**

### 5 3 Study site

We conducted field monitoring within the Ohya landslide in the Southern Japanese Alps (Fig. 2). The Ohya landslide has an estimated total volume of 120 million m<sup>3</sup>, and was initiated during an earthquake in A.D. 1707 (Tsuchiya and Imaizumi, 2010). The climate at the site is characterized by a high annual precipitation (about 3,400 mm) (Imaizumi et al., 2005). Heavy rainfall (i.e., total rainfall > 100 mm) occur during the rainy season from June to July and the autumn typhoon season (from August to October). The geological unit is Tertiary strata, which is composed of well-jointed sandstone and highly fractured shale. Unstable sediments have been supplied from outcrops into the channels in the landslide scar and have affected the initiation of debris flows since the original failure.

Almost all of debris flows in the Ohya landslide occur in the upper Ichinosawa catchment (Imaizumi et al., 2005). The total length of the channel is ≈650 m and the south-facing catchment (1,450 – 1,905 m a.s.l) has an area of 0.22 km<sup>2</sup>. Most of the basin is characterized by high and steep slopes (40 – 65°). Seventy percent of the slope is scree and outcrop, whereas the remaining 30% is covered with forest, shrubs, and tussocks. Anthropogenic influences are absent in the catchment because of the harsh environmental conditions.

Unconsolidated debris, ranging from sand particles to boulders (Imaizumi et al., 2016c), is located in the channel bed and talus cones, and is the source of debris flow material (Imaizumi et al., 2006). The thickness of debris deposits, including large

boulders ( $> 1$  m), exceeds several meters in some sections. Freeze-thaw that promotes dry ravel and rockfalls are the predominant sediment infilling of the channels (Imaizumi et al., 2006). Most of the channel was covered by sediment when a large volume of storage accumulated in the upper Ichinosawa, while bedrock exposed in some channel sections when the storage volume is low. Volume of storage displays seasonal changes caused by sediment supply from hillslopes in winter and early spring, and the evacuation of storage due to the occurrence of debris flow in summer and autumn (Imaizumi et al., 2006). The stored sediment has never been completely eroded by debris flows. Changes in the volume of storage at longer time scales (several years) occurs by the timing of large debris flows with a volume  $> 15,000$  m<sup>3</sup> that drastically decrease volume of storage (Imaizumi et al., 2016c).

10

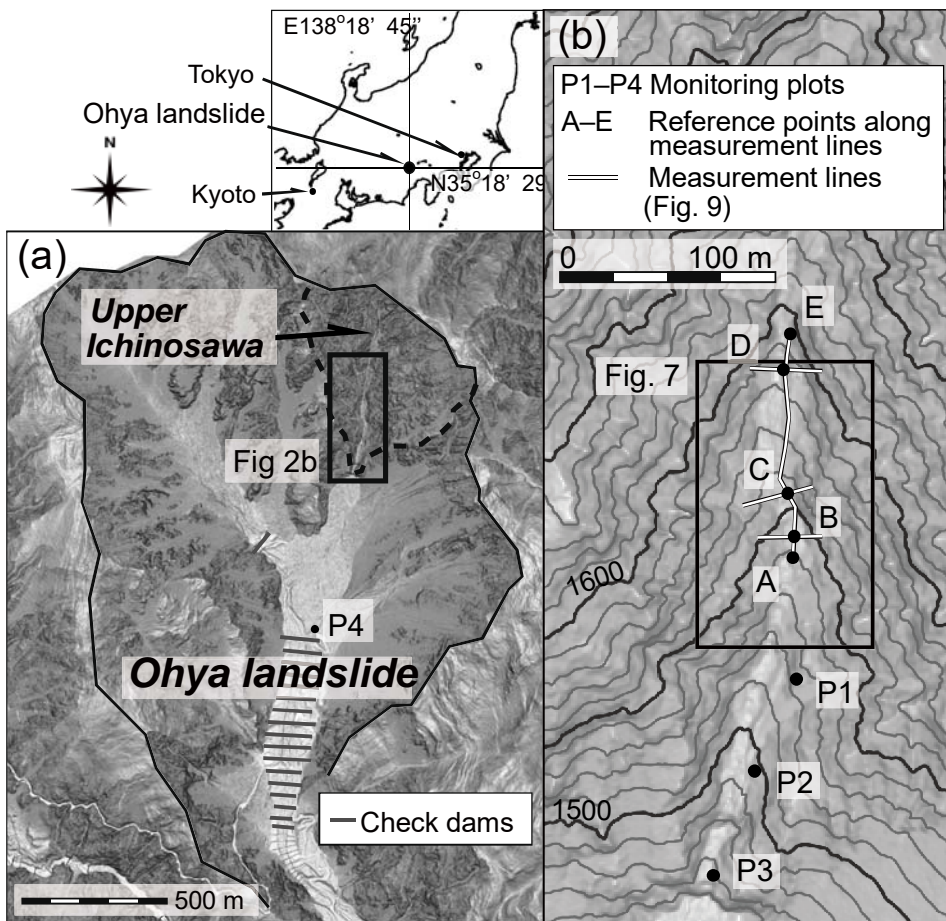


**Figure 2: Map of the Ohya landslide and upper Ichinosawa catchment: (a) Ohya landslide, (b) Ichinosawa upper catchment. Gentler and steeper terrains are expressed as light and dark colors, respectively.**

## 4 Methodology

### 4.1 Debris-flow Monitoring

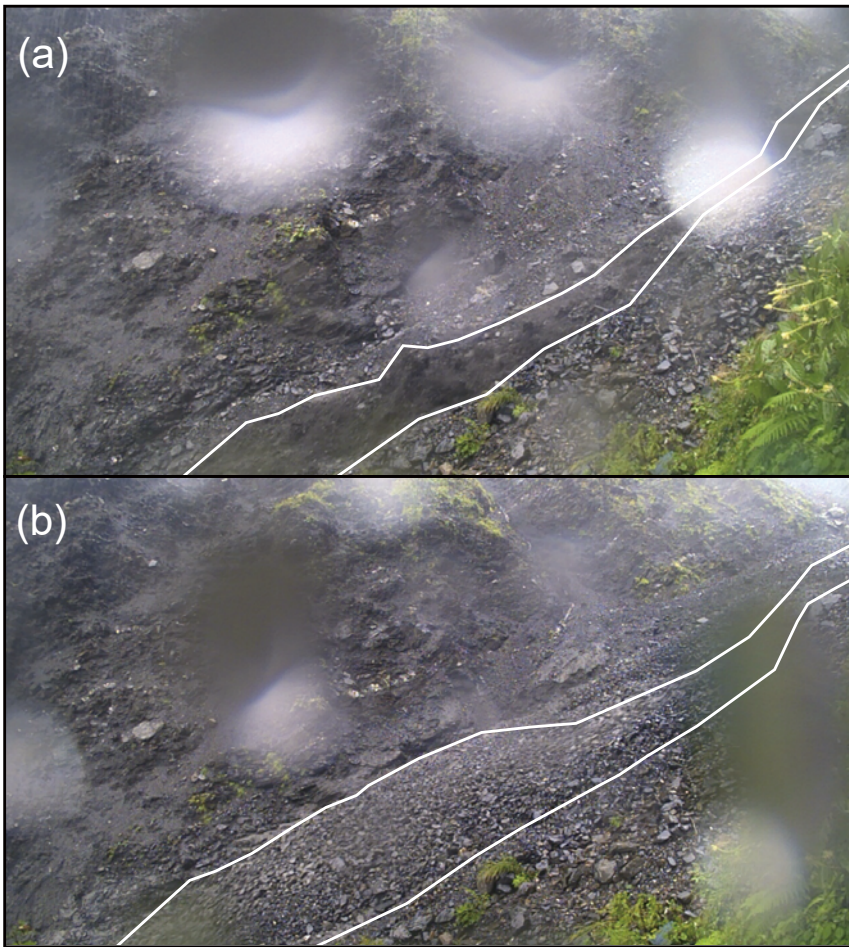
5 The monitoring system was installed in the study site in spring 1998 and consisted of a rain gauge, ultrasonic sensors, water pressure sensors, and a video camera (Imaizumi et al., 2005). The video camera, which provided motion images of debris flows, was initially monitored at P4, then moved to P2 in 2000 (Fig. 2). During the period of 1998 to 2001, the video camera was programmed to take 0.75 s clips of video every 5 min. In April 2001, this interval was shortened to 3 min to capture flow characteristics in more detail. In addition, continuous monitoring cameras, of which recording was initiated by wire motion  
10 sensors installed at several cross-sections in the channel, were initially installed at P1 in 2003, then at P3 and P2 in 2004 and 2005, respectively. The video camera system sometimes failed to capture debris flows because of their mechanical problems due to harsh site conditions. We identified timing of such debris flows by field surveys and water pressure sensors. Flow depth and surface velocity of debris flows at 1 second intervals were obtained from video image analysis. The surface velocity provided by the video image analysis does not represent the flow depth averaged velocity. The mean velocity was estimated  
15 from surface velocity multiplied by 0.6, based on the velocity profile throughout the flows on movable beds obtained from a physically based model by Takahashi (1977, 2014). Changes in cross-sectional area of flow were calculated from changes in flow depth and cross-section measurement of the channel topography. Discharge of debris flows were estimated from the cross-section area multiplied by mean velocity of all layers.

Imaizumi et al. (2006) classified the flow phases during debris flow events into two primary types: flows that made of  
20 mainly muddy water and those made of mainly cobbles and boulders. The former flows are turbulent and are characterized by black surfaces due to high concentrations of silty sediment sourced from shale in the interstitial water (Fig. 3a). Because the matrix of boulders is filled with interstitial water, this flow is considered fully saturated (Fig. 1d). In contrast, muddy water is not identified in the matrix of the flow surface of the second type of flow (Fig. 3b). Therefore, this type of flow is considered partly saturated (Fig. 1b). We visually identified temporal changes in the flow type during debris flow events from video  
25 images based on the existence of interstitial water on the flow surface.

Time-lapse cameras (TLCs; GardenWatchCam, Brino, Taipei City, Taiwan) were installed around P1 and P2 in April, 2013, as a backup for video camera monitoring. The number of cameras (1 to 6) differed among the various measurement periods. The intervals used for capturing images were also different among the measurement periods and for the various cameras, with a range from 1 s to 10 min.

30 To identify the arrival of debris flow, a semiconductor type water pressure sensors, which monitored hydrostatic pressures up to 49 kPa with an accuracy of  $\pm 3\%$ , were placed in holes dug in the bedrock of the channel bed. The logging interval was set at 1 min. Because water pressure sensors were sometimes washed away by debris flow, ultrasonic sensors with a measuring

range from 120 to 600 cm (accuracy of  $\pm 0.4\%$ ) were installed to monitor the surface height of debris flows at 1 min intervals as the backup of water pressure sensors. Water pressure and flow height monitored by these instruments showed intense and abrupt changes during the passage of debris flows, whereas such changes were absent during rainfall-runoff events without occurrence of debris flow. Therefore, we used water pressure and flow depth to identify the occurrence of debris flows.



5

**Figure 3: Images of fully and partly saturated debris flows captured by a TLC at plot P2 in Fig. 2. (a) Fully saturated debris flow captured 9 September 2015, 8:41 (LT). (b) Partly saturated debris flow captured at 9 September 2015, 7:43 (LT). Cobbles and boulders covers flow surface of the partly saturated debris flow (Imaizumi et al., 2016b).**

#### 10 4.2 Topographic Data Obtained by TLS

To clarify temporal changes in the micro channel bed topography associated with occurrence of debris flows, a TLS unit (GLS-1500 Topcon Co., Tokyo, Japan) was used to measure the topography of valley axis (Fig. 2) (Hayakawa et al., 2016). The maximum measurable distance of the TLS unit is 500 m (for target objects with a 90% reflectance), with accuracies of 6'' for

angle and 4 mm for distance (at 150 m range). From November 2011, field measurements were undertaken in spring, summer, and autumn for 4 years (Table 1). For each measurement, the scanner was set at two positions. One was at the downstream side of the target area (P1 in Fig. 2), where the land had been relatively stable for many years. The other at the upstream side of the target area (around point D in Fig. 2). The location of this scan position varied with time because it was in the valley bottom where the topography changed due to erosion and deposition by debris flows. The point clouds measured from different scan positions were registered using at least five reference targets placed between the two scan positions. The two point clouds were registered by the target matching method using these reference targets, with accuracies of 0.5–6 mm. The geographic coordinates (Japan Plane Rectangular CS VIII, EPSG: 2450) of two targets, selected as georeference points, were measured with global navigation satellite system (GNSS) receivers (GeoXH 6000, Trimble, Sunnyvale, CA, USA or GRS-1, Topcon Co., Japan; accurate to a range of 10–63 mm in XY or Z). The baseline solution was calculated using data from GNSS base stations of GEONET, the Japanese GNSS network operated by the Geospatial Authority of Japan. The overall uncertainties of the point clouds, including scanning, registration, and georeferencing by GNSS, were considered in the order of centimeters to a decimeter (Hayakawa et al., 2016).

15 **Table 1: Date of TLS survey**

Year	Date of survey	Number of debris flow after previous scanning	Date of last debris flow event* <sup>1</sup>
2011	November 11	-	October 14
2012	May 14	0	-
	August 23	2	June 22
	November 21	3	September 30
2013	May 10	0	-
	August 16	0	-
	November 19	2	September 15
2014	May 16	0	-
	August 17	1	August 10
	November 28	2	October 5
2015	May 15	0	-
	August 23	4	August 17
	December 4	1	September 9

\*1 Date of the last debris flow event are not listed when debris flow had not occurred in the year, because the topography was possibly affected by the winter sediment supply rather than the last debris flow in the previous year.

20 After manually eliminating noise and unnecessary points, the point clouds obtained by the TLS measurement were converted into digital elevation models (DEMs) using a simple linear interpolation by triangulated irregular network (TIN) and resampling, because vegetation cover was absent in the site. The resolution of the DEMs was set at 10 cm, which sufficiently covers the average point density of the point clouds. Areas with sparse point clouds (approximately <math><100\text{ point m}^{-2}</math>), vegetated areas, and

areas affected by the combination of various processes (e.g., talus slopes with the lower part eroded by stream flow) were excluded from the analyses.

The extent of typical geomorphic units in the TLS survey area, including three rock slopes, three talus slopes, and a channel around the monitoring plot P1, was mapped by field surveys to calculate the slope gradient of geomorphic units with various grid sizes (Fig. 4). The mapping was conducted at the same time as each TLS survey because the area changed over time due to the sediment supply from outcrops and transportation of sediment by debris flows.



**Figure 4: Photograph of the typical geomorphic units seen from P1. The image shows the area of rock slopes (surrounded by red lines), talus slopes (surrounded by yellow lines), and a channel (surrounded by blue lines), for which the slope gradient was calculated from DEMs with various grid sizes. The numbering of the area corresponds to that used in Fig. 7.**

#### 10 4.3 Estimation of debris-flow volumes

We estimated the volume of storage from photographs taken periodically at sites P1 and P4 (Fig. 2) (Imaizumi et al., 2016a). We could not use data obtained by periodical TLS, because the target area of the TLS was a fraction of the storage zone. Photographs from site P4 cover the entire study site, whereas those from P1 focus on channel deposits at the bottom of the incised main channel, which is shaded in photographs from P4. By comparing these photographs with catchment topography and ortho photographs, which are obtained by airborne laser scanning (ALS) in seven periods (2005, 2006, 2009, 2010, 2011, 2012, and 2013), the area covered by storage (i.e., channel deposits and talus slopes) in each photograph periods was mapped on GIS. The bedrock topography in the upper Ichinosawa catchment was estimated from terrains by ALS in the periods when sediment storage was almost absent (i.e., in 2011 and 2012). Thirty-three cross-sectional areas of the storage with spacing of 25 m along the channels (24 cross-sections along the main channel and 9 cross-sections along a tributary) were calculated from the bedrock topography estimated from terrains by ALS and the location of both ends of the storage along the cross-sections on the GIS storage map under the assumption that surface topography of the storage was an inclined line connecting both ends of the storage. Total volume of the storage was calculated by sum of the cross-sectional area multiplied by the spacing of cross-

sections (25 m). The root mean squared error (RMSE) of the procedure, which was obtained from comparison of the volumes of storage by the procedure and that by subtraction of ALS DEMs by estimated bedrock topography, was 5361 m<sup>3</sup> (Imaizumi et al., 2016a). This RMSE is larger than the volume of small debris flows (<2000 m<sup>3</sup>) but below the sediment supply volume in each year (>10,000 m<sup>3</sup>).

## 5 Results

### 5.1 Debris flow monitoring

From 1998 to 2015, 59 debris flows, which went through or terminated in the reach between the sites P1 to P3, were observed by video cameras, field surveys, and water pressure sensors in the upper Ichinosawa catchment. In addition, the occurrence of some other debris flows, which terminated above site P1, were found by periodic photography and field surveys. We analyzed video images of seven flows that were clearly captured by video cameras. In addition, we analyzed photographs of one debris flow taken by TLCs with an interval of 1 s (Table 2). We failed to obtain clear video images of other debris flows because of darkness at night and fog. Most of the rainfall events triggering debris flows in the study site can be classified into two groups: long-lasting rainfall events with high value of total rainfall depth, caused by typhoons and stationary fronts (rainfall duration >5 h and total rainfall >50 mm), and short-duration convective rainfall events characterized by high intensity (rainfall duration <5 h, total rainfall <50 mm; Table 2).

As noted above, two types of flow have been observed in the Ohya landslide: flow mainly composed of cobbles and boulders (partly saturated flow) and flow mainly composed of muddy water (fully saturated flow). The duration of each flow phase varied between the events. For example in the event of 5 August 2008, 88% of debris flow surges (percentage respect to the total event duration) was composed of partly saturated flow, while in the event of 30 August 2004 (Fig. 5), 90% in time of the phenomenon was composed of fully saturated flow. The proportional duration of the partly saturated debris flow in overall debris flow surges had a weak positive relationship with the volume of storage estimated from periodical photography ( $R^2 = 0.37$ ,  $p$ -value = 0.06; Fig. 6). Rainfall was also a potential factor controlling flow type. The proportion of fully saturated flow respect to the total event duration was generally high during long-lasting rainfall events associated with typhoons and stationary fronts, while the proportion of partly saturated flow was high during short-time convective rainfall (Fig. 6, Table 2). The  $p$ -value for the difference in the proportional duration of the flow types between the two rainfall typology was below 0.01.



**Table 2: Details of the rainfall and flow types during the debris flow events analyzed in this study**

Date	Total rainfall (mm)	Maximum 10-min. rainfall intensity (mm/10min.)	Rainfall duration	Rainfall type	Type of camera	Location of camera	Proportional duration of partly saturated flow in overall debris flow surges
30 August 2004	276.5	7.5	31 h 50 min.	Typhoon	Video	P3	0.10 <sup>*a</sup>
19 July 2006	178.0	5.5	37 h 10 min.	Stationary front	Video	P2	0.65
6 September 2007	501.5	9.5	37 h 30 min.	Typhoon	Video	P2	0.49 <sup>*a</sup>
5 August 2008	39.5	13.5	1 h 30 min.	Convective	Video	P2	0.88
24 July 2010	21.0	13.0	1 h 10 min.	Convective	Video	P2	1.00
30 September 2012	86.0	6.5	7 h 40 min.	Typhoon	Video	P3	0.23 <sup>*a</sup>
6 August 2015	44.5	21.0	1 h 50 min.	Convective	Video	P1	0.99
9 September 2015	203.0	8.0	36 h 50 min.	Typhoon	TLC	P1	0.42

\*a Latter half of the debris flow event was not analyzed because of the darkness affected by the sunset. Therefore, latter half of the event is not included in this data.

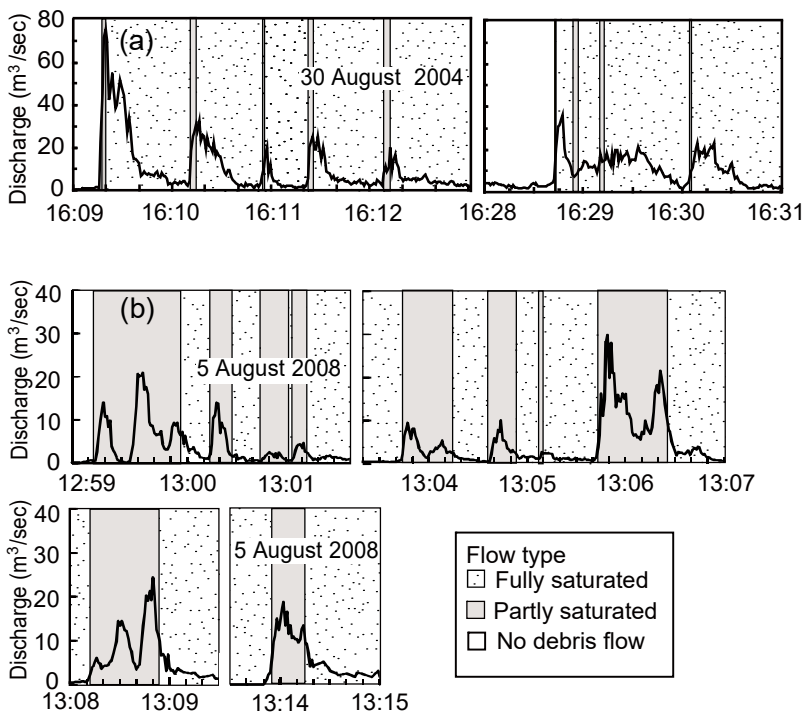


**Figure 5: Hydrograph and the duration of each flow type during debris flow events. (a) Debris flow on August 30, 2004, mainly consisting of fully saturated flow. (b) Debris flow on August 5, 2008, mainly consisting of partly saturated flow.**

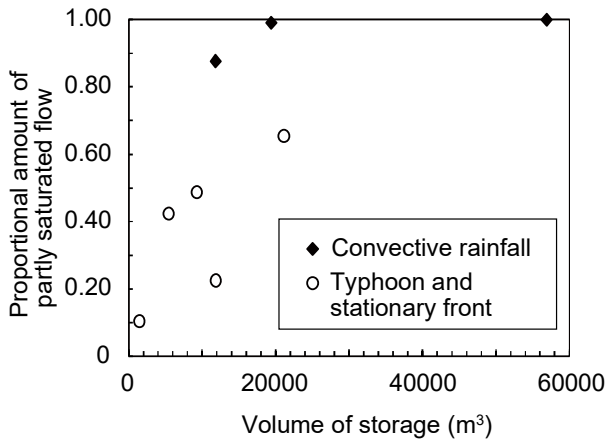


**Figure 6: Comparison between the volume of storage and the duration of partly saturated flow as a proportion of the overall debris flow surges.**

## 5.2 Slope gradient of geomorphic units

5 Mapping of the three geomorphic units (rock slopes, talus slopes, and the channel) in the TLS survey area showed that the location of each unit was largely similar throughout the study periods, while the size of each unit changed due to sediment supply and transport processes. Some talus slopes completely disappeared in several periods because of erosion by debris flows. Slope gradient was calculated using 3x3 neighbourhood around each cell in the DEM with various grid size obtained by TLS (Horn, 1981; Fig. 7). On the slope gradient map with a grid size of 0.1 m, the slope gradient is spatially variable  
 10 attributable to boulders at a scale on the order of decimetres (Fig. 7). Step-pool-like topography with a height of several meters formed by large boulders (>1.0 m) and bedrock morphology was visible in the channel on the slope gradient maps with a grid size of  $\geq 1.0$  m (Fig. 7).

Average and standard deviation of slope gradient in the three geomorphic units (rock slopes, talus slopes, and the channel) throughout the TLS monitoring period were calculated from DEMs with various grid size. Regardless of the grid size, the  
 15 average slope gradient of rock slopes and the channel were the highest and lowest among the three geomorphic units, respectively (Fig. 8a). The average slope gradient of each geomorphic unit becomes gentler with an increase in the grid size (Fig. 8a). However, the relationship between grid size and slope gradient was slightly different among geomorphic units. For a grid size of  $\geq 1.0$  m, a histogram of the slope gradient in talus slopes was concentrated in a narrow range around the average value (i.e., >60% in the range between 34–40° for a grid size of 5.0 m; Fig. 8b). This slope angle is considered to represent  $\alpha_1$ ,  
 20 as reported in previous studies (Kirkby and Statham, 1975; Carson, 1977; Obanawa and Matsukura, 2008). The standard deviation of the slope gradient in the rock slope decreased with an increase in grid size when the grid size was smaller than the width of alternative strata in the study area (about 4.0 m; Imaizumi et al., 2015), and was almost constant when the grid size was larger than that. The standard deviation of the slope gradient in the channel also decreased with an increase in grid size when the grid size was smaller than 4.0 m, and was almost constant when the grid size was larger than 4.0 m. This inflection

point of the trend (4.0 m) was the larger than the largest boulder size in the channel, changing with time from 1 to 2 m (Imaizumi et al., 2006; Imaizumi et al., 2016c).

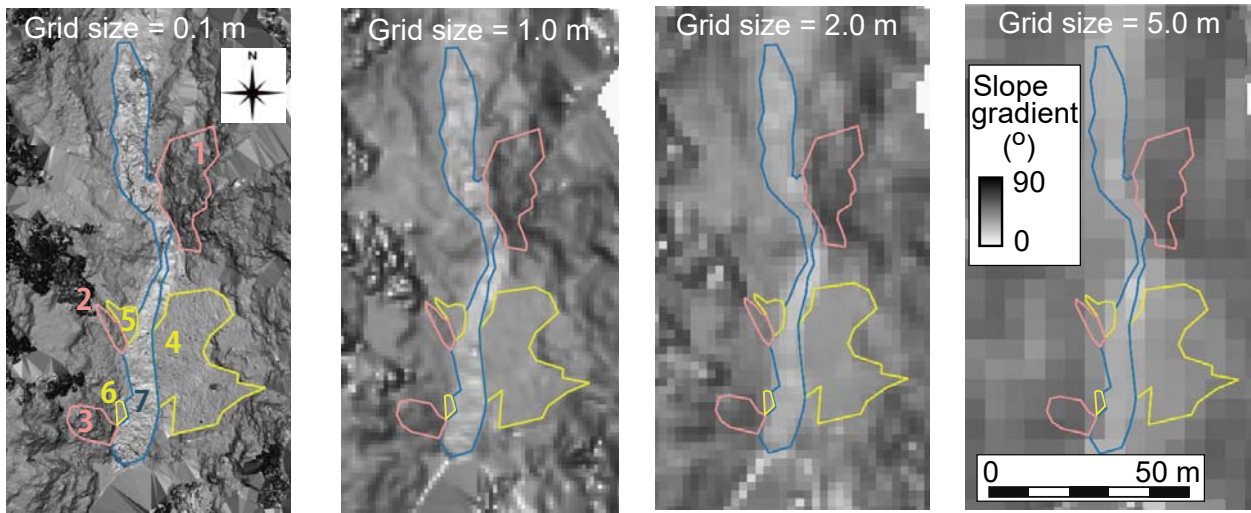
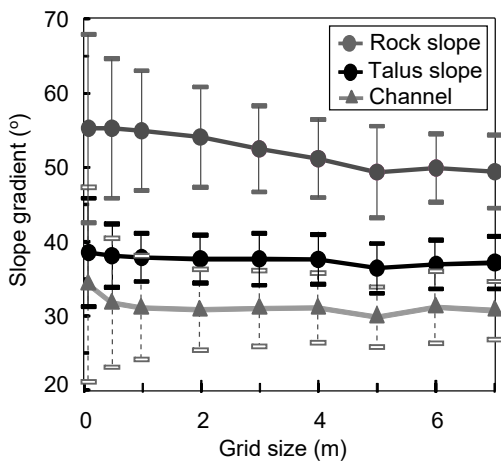


Figure 7: Slope gradient map calculated after using terrestrial laser scanning (TLS) data on 14 May 2014, with various grid sizes. The location of the analysis area is shown in Fig. 2.

5

(a) Average slope gradient



(b) Histogram

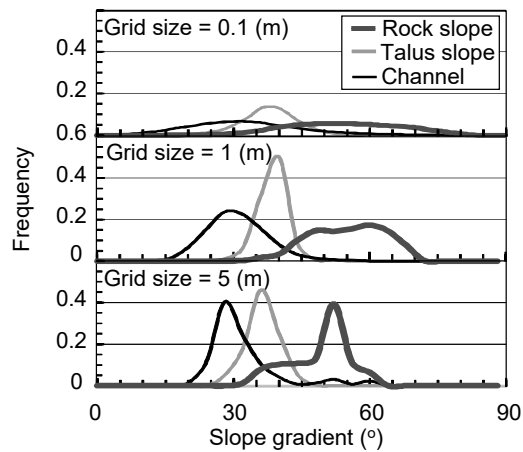


Figure 8: Slope gradient of typical geomorphic units calculated from terrestrial laser scanning (TLS) derived digital elevation maps (DEMs) with various grid sizes. Topographic data in all measurement periods were used in the statistical analysis. (a) Changes in the average slope gradient of each geomorphic unit with an increase in the grid size. The slope gradient in all periods was averaged. The bars attached to the plots indicate the range of the standard deviation. (b) Histogram of the slope gradient calculated from TLS DEMs, with grid sizes of 0.1, 1.0, and 5.0 m.

10

### 5.3 Longitudinal channel topography

Longitudinal channel profiles obtained by the post-event surveys were analysed by GIS to find out the relationship between the debris flow characteristics and channel topography (i.e., channel gradient) formed by the debris flow in the steep debris-flow initiation zone (Fig. 9). The channel topography between points A and E (total length of 100 m; Fig. 2) on 21 November 2012 was mainly formed by a debris flow on 30 September 2012, which was dominated by fully saturated flow. In contrast, the channel topography on 23 August 2015, was mainly formed by a debris flow on 6 August 2015, which was dominated by partly saturated flow. A small debris flow on 17 August 2015, which transported storage with a volume of  $<3,000 \text{ m}^3$ , also affected a part of the channel topography measured on 23 August 2015; however, the affected area was limited (mostly a width of  $<5 \text{ m}$ ) because of its small discharge. Thus, we assumed that the channel profile in the survey section on 23 August 2015 reflected characteristics of the debris flow on 6 August 2015, rather than that on 17 August 2015.

When we compared channel bed profiles on 21 November 2012 and 23 August 2015, the channel bed level was clearly different ( $>3 \text{ m}$  in depth) at the lowermost and uppermost reaches (within 25 m and from 75 to 90 m upstream of point A, respectively). In contrast, there was almost no change in the longitudinal channel profile ( $<1 \text{ m}$ ) in the middle reaches (within 30 m upstream of point C). Such differences in channel bed deformation could also be identified in the cross-sectional profile. The cross-sectional profile at the lowermost and uppermost reaches (points B and D, respectively) was clearly different, while difference in the profile was not apparent at the middle reaches (point C; Figs. 9e, 9f, 9g). Channel topography after many other debris flows in our monitoring site showed similar trend that the channel bed deformation in the lowermost and uppermost reaches was active, in contrast to the inactive riverbed deformation in the middle reaches (Hayakawa et al., 2016).

The longitudinal profile of the channel gradient differed among debris flow events. The distribution of the channel gradient calculated for each 0.1 m section (the scale of a boulder) on November 21, 2012 (mainly formed by fully saturated flow), was clearly wider than that on 23 August 2015 (mainly formed by partly saturated flow; Fig. 9b, Table 3a). The p-value obtained by an F-test of the difference in the dispersion of the channel gradient between the two periods was  $<0.001$ . In contrast, the average slope gradient in the section between A and E was not significantly different between the two periods ( $23.1^\circ$  and  $25.4^\circ$  for 21 November 2012, and 23 August 2015, respectively).

The difference in the amplitude of the channel gradient calculated for each 1.0 and 5.0 m section was also clear (Figs. 9c, 9d, Table 3a). The p-values obtained by an F-test of the difference in the dispersion of the channel gradient between the two periods was  $<0.001$  and  $<0.05$  for each 1.0 and 5.0 m section, respectively. Such temporal changes in the channel gradient was more evident in the sections with active channel bed deformation (from 0 to 25 and from 75 to 90 m from point A) compared to those without active channel bed deformation (from 25 to 75 and from 90 to 100 m from point A) (Tables 3b, 3c). Wide distribution of the slope gradient for each 5.0 m section on 21 November 2012 was mainly attributed to the step-pool topography formed by large boulders and the bedrock step-pool, while that for each 1.0 m section was attributed to such small-scale topographies together with the particle size of large boulders. The cross-sectional topography in the reaches without active channel bed deformation was narrowed by the massive and steep rock cliffs at the left bank (right side of the point C in

Fig. 9f). High stream power attributed to the high flow depth in this section possibly restricted deposition of the sediment, resulting in inactive channel bed deformation.

Periodic photography and field surveys after eight debris flows, which were successfully monitored by video cameras and TLCs, indicated that small-scale topography after debris flows mainly consisting of fully saturated flow are rugged compared to that after debris flows mainly consisting of partly saturated flow. This trend agrees with that observed by TLS surveys (Fig. 9, Table 3a).

The standard deviation of the channel gradient in the active channel bed deformation sections had a negative relationship with the volume of the storage (Fig. 10a). The p-values for the linear regressions with section lengths of 0.1, 1.0, and 5.0 m were <0.1, <0.05, and <0.05, respectively.

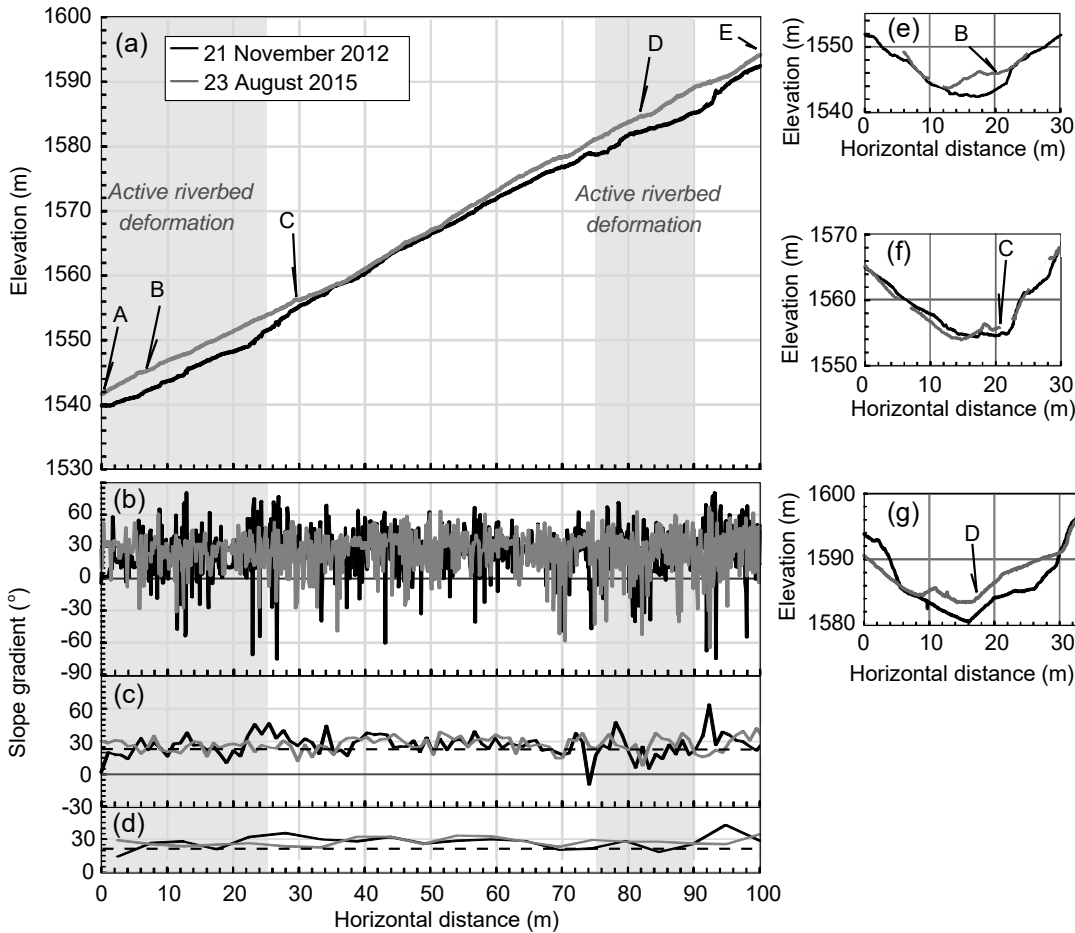


Figure 9: Channel profiles and channel gradient mainly formed by fully saturated flow (measured on 21 November 2012 after the debris flow on 30 September 2012) and partly saturated flow (measured on 23 August 2015 after the debris flow on 6 August 2015), obtained from 0.1 m terrestrial laser scanning (TLS) derived digital elevation maps (DEMs). (a) Longitudinal channel profile in the section between A to E in Fig. 2. (b) Longitudinal changes in the channel gradient calculated for each section with a length of 0.1 m. (c) Longitudinal changes in the channel gradient calculated for each section with a length of 1.0 m. (d) Longitudinal changes in the

channel gradient calculated for each section with a length of 5.0 m. (e) Cross-sectional profile of the channel at point B. (f) Cross-sectional profile of the channel at point C. (g) Cross-sectional profile of the channel at point D. Data at some cross-sections on 9 August 2015, are absent because of the failure of the TLS survey due to the weather conditions (panels e and f).

5 **Table 3 Standard deviation of the channel gradient and proportional amount of channel sections in which the gradient was in the range between  $\alpha_2$  and  $\alpha_1$  throughout the entire channel section.**

(a) Entire channel section between points A to E

Measurement date	Standard deviation of the channel gradient			Proportion of all sections between $\alpha_1$ and $\alpha_2$		
	0.1 m interval	1.0 m interval	5.0 m interval	0.1 m interval	1.0 m interval	5.0 m interval
21 November 2012	23.7	10.3	5.8	0.31	0.52	0.80
23 August 2015	18.7	7.0	3.7	0.38	0.73	0.95

(b) Sections with active channel bed deformation (from 0 to 25 and from 75 to 90 m from point A).

Measurement date	Standard deviation of the channel gradient			Proportion of all sections between $\alpha_1$ and $\alpha_2$		
	0.1 m interval	1.0 m interval	5.0 m interval	0.1 m interval	1.0 m interval	5.0 m interval
21 November 2012	27.0	11.4	6.3	0.30	0.38	0.44
23 August 2015	17.9	7.2	3.4	0.48	0.71	0.89

(c) Sections without active channel bed deformation (from 25 to 75 and from 90 to 100 m from point A).

Measurement date	Standard deviation of the channel gradient			Proportion of all sections between $\alpha_1$ and $\alpha_2$		
	0.1 m interval	1.0 m interval	5.0 m interval	0.1 m interval	1.0 m interval	5.0 m interval
21 November 2012	20.9	8.6	5.1	0.34	0.61	0.90
23 August 2015	18.8	6.5	3.5	0.33	0.76	1.00

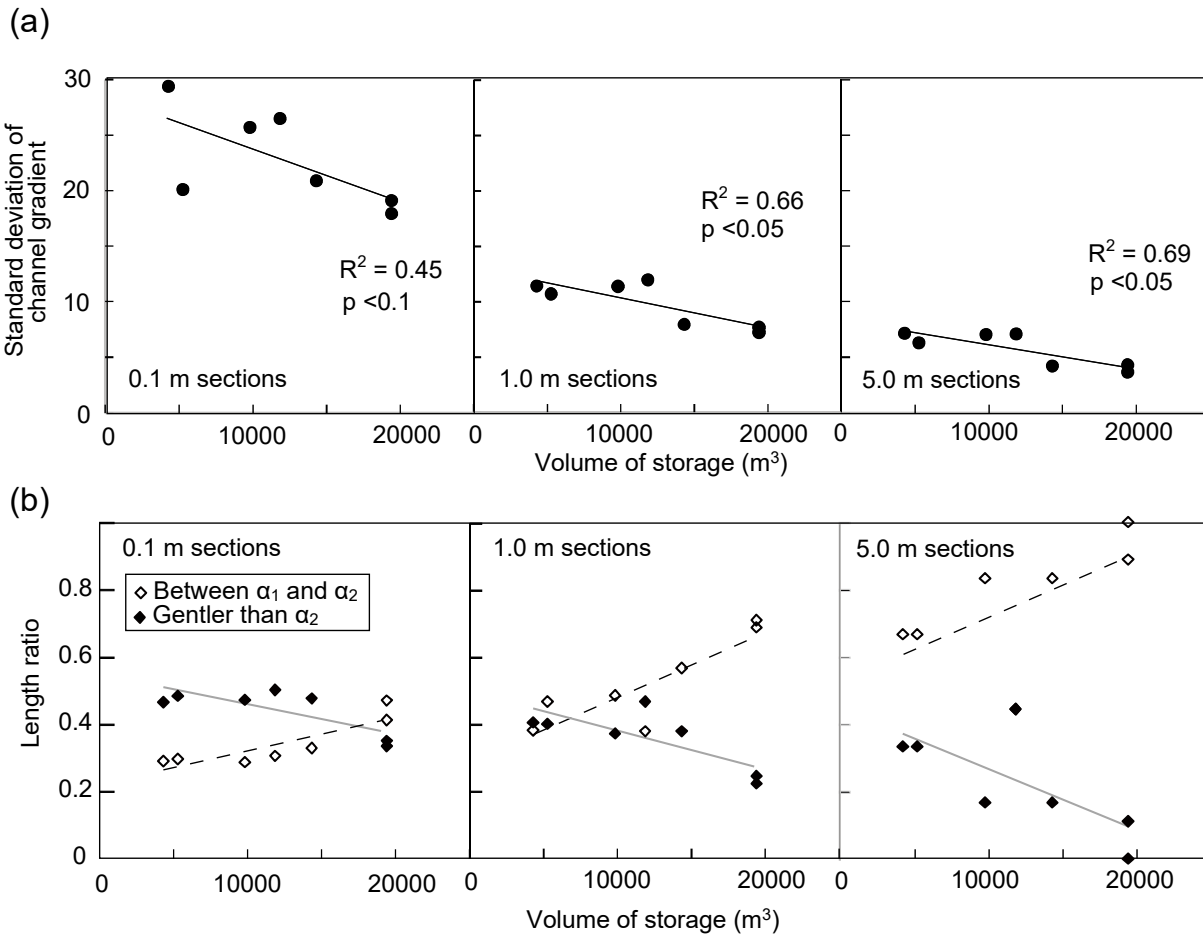


Figure 10: Comparison between the volume of storage and channel topography. (a) Comparison of the volume of storage with the standard deviation of the channel gradient for each 0.1, 1.0, and 5.0 m section in the active channel bed deformation zones (from 0 to 25 m and from 75 to 90 m upstream of point A). (b) Comparison of the volume of storage with the length of the channel sections, in which the channel gradient ranged between  $\alpha_1$  and  $\alpha_2$  (theoretical channel gradient for partly saturated debris flow) and gentler than  $\alpha_2$  (theoretical channel gradient for fully saturated debris flow), in the active channel bed deformation zones. Topographic data before the first debris flow in each year were excluded from the analyses, because the channel gradient was possibly affected by the sediment supply from hillslopes, as well as the last debris flow of the previous year. The topography on August 17, 2014, was also excluded from the analysis because we failed to measure topography by terrestrial laser scanning (TLS) in the upper part of the active channel bed deformation zones because of fog. Linear regression lines for each relationship are also shown in the figure.

5

10 As noted above, the theoretical channel gradient dividing partly and fully saturated debris flows ( $\alpha_2$ ) can be obtained from Eq. (5). Because the dispersion of boulders in the partly saturated debris flows was not evident in video images, porosity (ratio of liquid and vapor phases, to be exact) in the partly saturated flow may not be higher than that in the saturated channel deposits. By assuming  $\phi = 37.3^\circ$  (average slope gradient of the talus slope for a grid size = 1.0 to 7.0 m),  $n = 0.3$  (same as the porosity of channel deposits),  $\gamma_s = 26000$ , and  $\gamma_w = 9800$ , the  $\alpha_2$  in the Ohya landslide was  $22.2^\circ$ . When we focused on the channel

15 sections with active channel bed deformation, the proportional amount of channel sections in which the gradient was in the range between  $\alpha_2$  and  $\alpha_1$  (theoretical channel gradient for partly saturated flow) in the entire channel section on 23 August

2015 (after mainly formed by partly saturated flow) was higher than on 21 November 2012 (after mainly formed by fully saturated flow), regardless of the interval of channel section for the analyses (Table 3b).

The proportional amount of all channel sections, in which the gradient was in the range between  $\alpha_2$  and  $\alpha_1$ , throughout the entire channel section with active channel bed deformation was higher when the volume of storage was large (Fig. 10b). The relationship was clear for all 0.1, 1.0, and 5.0 m section lengths ( $p$ -value  $< 0.05$ ). In contrast, the proportional amount of all channel sections, in which the channel gradient was gentler than  $\alpha_2$ , throughout the entire channel section decreased with an increase in the volume of sediment storage. The gradient of the regression line for the section length of 0.1 m was gentler than that for the section lengths of 1.0 and 5.0 m.

## 6. Discussion

### 6.1 Factors controlling the debris flow type

In contrast to debris-flow transportation zones in other torrents, in which partly saturated flow dominates just at the front of surges (McArdell et al., 2007; McCoy et al., 2010; Okano et al., 2012), our observations in the debris flow initiation zone of the upper Ichinosawa showed that partly saturated flow sometimes dominates the entire debris flow (Table 2). Many sections in the upper Ichinosawa catchment are greater than  $22.2^\circ$  (Fig. 9), which is the theoretical channel gradient needed for occurrence of a partly saturated debris flow in the Ichinosawa catchment. Although the  $\alpha_2$  is different among torrents affected by soil parameters such as the internal angle of friction, debris flow initiation zones in other torrents, which are generally greater than  $22.2^\circ$  (e.g., VanDine 1985; McCoy et al., 2012), possibly satisfy the conditions for the occurrence of partly saturated flow.

The proportional duration of partly saturated flow in the overall surges had a positive relationship with the volume of storage (Fig. 6). Thus, the volume of storage was a factor controlling not only the initiation of the debris flow, particularly in the supply limited basin (Bovis and Jakob, 1999; Jakob et al., 2005), but also the debris flow characteristics. The water content in the storage, which is considered an important factor controlling flow characteristics (Takahashi, 1991; Hürlimann et al., 2015), may affect such relationships. When a large volume of storage is present in a basin, a large amount of water is needed for saturation of the storage, which can be difficult to attain. In such cases, even if the sediment mass that initially moved in the channel was saturated, storage along the channel eroded by the debris flow would not be fully saturated when the channel gradient  $> \alpha_2$ . Consequently, partly saturated flow can easily dominate when a large volume of storage accumulates in the channel. Such erosion of unsaturated sediment has also been reported in other channels (Berger et al., 2011b; McCoy et al., 2012). In contrast, storage can be easily saturated by smaller amounts of rainfall when there is only a small volume of storage in the basin. Thus, even when debris flows were not fully saturated in their initial stages, as they traveled downstream they easily became saturated by the water supply from tributaries as well as the erosion of saturated deposits.

Our monitoring results also revealed that the proportional duration of partly saturated flow in a debris flow event was low during long-lasting rainfall events (e.g., typhoons and stationary fronts), while the duration was high during short-lasting



rainfall events (e.g., convective rainfall; Table 2, Fig. 6). The relationships between rainfall patterns and flow characteristics have also been reported in other debris flow basins (Okano et al., 2012; Kean et al., 2013; Hürlimann et al., 2014). Okano et al. (2012) obtained a similar trend to that found in Ichinosawa catchment based on observations in the transportation zone. The front of a surge was completely saturated when rainfall intensity over a long duration (24 h) was high, while partly saturated flow occurred at the front of surges during short-term, intense rainfall events. Such a relationship between flow type and rainfall pattern can also be explained by the water content in the storage. During long-lasting rainfall events with high levels of cumulative rainfall, the amount of water in the storage can be high, resulting in a predominance of saturated flow. Water supply from tributaries during such long rainfall events also increases the water content in the debris flow (Okano et al., 2012). In contrast, the amount of water in the storage may be low during short-duration rainfall events with low levels of cumulative rainfall, resulting in the domination of partly saturated flow. Consequently, both amount of water supplied by rainfall and that of sediment storage need to be known when we consider water contents in the material affecting the debris flow type. Previous study reported changes in the flow characteristics during a debris flow event associated with the sediment supply from hillslopes (Staley et al., 2014; Zhou et al., 2015), possibly because of the increasing in the amount of sediment relative to the water in channels.

## 15 **6.2 Influence of the sediment transport type on the slope gradient of terrains**

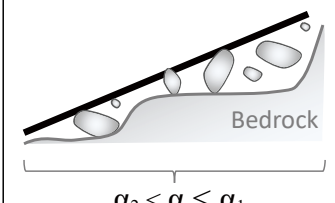
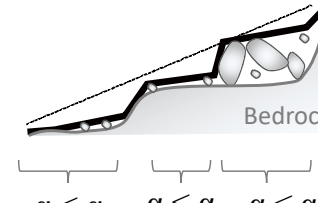
The value of topographic indexes (e.g., slope gradient) are variable depending on the scale of the window size used in the GIS analyses, because factors affecting the indexes are different among the scales of topography (Schmidt and Andrew, 2005; Pirotti and Tarolli, 2010; Drăguț and Eisank, 2011). In order to figure out appropriate window size for the analysis of the sediment transport type, we compared histograms of the slope gradient calculated with various window sizes each other (Fig. 8). As a result, the peak of the histogram of the slope gradient for each geomorphic unit was steep and high when the grid size was sufficiently large to eliminate the influence of small-scale roughness attributed to particle size (Fig. 8b). For example, histogram for the talus slope was steep when grid size was  $\geq 1.0$  m, which was larger than the maximum grain size of boulders on talus slopes (0.5 m). Histogram for the channel with grid size of 5.0 m was steeper and higher than that with grid size of 1.0 m, possibly affected by the size of the largest boulders in the channel, changing from 1 to 2 m associated with the sediment supply from hillslopes and sediment transport by debris flows (Imaizumi et al., 2006; Imaizumi et al., 2016c). Thus, when we analyse relationship between the type of sediment transport and the slope gradient of terrains, window size larger than the particle size, which can eliminate roughness attributed to the particle size, would be appropriate, because the particle size is considered to be not directly affected by the sediment transport type.

A large part of the histogram of the rock slopes was steeper than  $40^\circ$  for a grid size of  $>4.0$  m (e.g., 80% for a grid size of 5.0 m; Fig. 8b), indicating that fully unsaturated sediment transport, which occurs on slopes steeper than  $\alpha_1$  (Eq. (4)), is dominant on rock slopes. In contrast, most of the channel was gentler than  $\alpha_1$  for a grid size of  $>4.0$  m (e.g.,  $>85\%$  for a grid size of 5.0 m; Fig. 8b), indicating that fully and partly saturated debris flows are dominant in the channel. Such a trend was also apparent in the longitudinal profile of the channel (Fig. 9b). Based on the statistics of the channel gradient for each 5.0 m

channel section, the sum of the length ratio of the channel sections in the theoretical range of fully and partly saturated debris flows was almost 1.0.

The longitudinal channel gradient changed with time and was affected by the predominant type of flow during the preceding debris flow events (Fig. 9). The proportional amount of channel sections between  $\alpha_1$  and  $\alpha_2$  (theoretical range of the channel gradient for partly saturated debris flow) among all active channel deformation sections was higher when a larger volume of storage was present in the catchment (Fig. 10b). Because partly saturated flow dominated when a large volume of storage was present in the catchment (Fig. 6), partly saturated debris flow likely formed channel topographies with a theoretical channel gradient for the partly saturated flow (Fig. 11). Similarly, the length of the channel sections in the theoretical range for fully saturated flow ( $<\alpha_2$ ) was high when small amounts of storage accumulated in the channel (Fig. 10b), during periods when fully saturated flow dominated (Fig. 6). Thus, fully saturated flow tended to form channel sections gentler than  $\alpha_2$  (Fig. 11). The standard deviation of the channel gradient after a debris flow mainly consisting of fully saturated flow was higher than that after a debris flow mainly consisting of partly saturated flow (Fig. 8, Table 3). In addition, the standard deviation of the channel gradient was high when small volumes of storage accumulated in the basin (Fig. 10a), implying that fully saturated flow tended to form a step-pool topography. Such trend was clear in the window size eliminating roughness attributed to the particle size of large boulders (i.e., 5.0 m sections). As a result of field surveys and periodic topography, step-pool topography formed by large boulders and the bedrock was generally seen after fully saturated flows. Since temporal changes in the channel gradient were not apparent in the larger-scale topography (i.e., channel gradient for entire sections with an active riverbed deformation with a length of 40 m), the decrease in the channel gradient due to fully saturated flow did not occur throughout the channel but was occasionally interrupted by steep sections formed by large boulders and bed rock, which cannot be eroded easily (Fig. 11).

Because we did not consider the dynamic mechanisms of the debris flow, including the collision of particles and the dynamic pressure of interstitial water (Coussot and Meunie, 1999; Takahashi, 2014), our analysis could not discuss unsteady nature of debris flows, such as temporal changes in the flow type during a debris flow event. In addition, temporary appearance of the unsaturated (or extremely dense) debris flows in gentler torrents does not agree with our analysis of static force (McArdell et al., 2007; McCoy et al., 2013; Okano et al., 2012). Depth profile of the dynamic force affected by the slope gradient and the particle size relative to the flow depth should be considered to complete explanation of such dense debris flows (Takahashi, 2007; Lanzoni et al., 2017). Nevertheless, our analysis results suggested that rough relationships between the predominant types of sediment transport and the slope gradient exist in the debris flow initiation zone.

Volume of storage	Large	Small
Flow type	Mainly composed of <u>partly</u> saturated flow	Mainly composed of <u>fully</u> saturated flow
Channel topography		

**Figure 10: Schematic diagram of the relationships between the volume of storage, flow type, and channel topography.  $\alpha$  is the channel gradient,  $\alpha_1$  is the theoretical boundary of the channel gradient between fully unsaturated and partly saturated sediment transport, and  $\alpha_2$  is the theoretical boundary of the channel gradient between partly and fully saturated sediment transport.**

## 5 7 Summary and conclusion

We investigated the interaction between flow characteristics and topography in the debris flow initiation zone at the Ohya landslide, Japan, using various methods, including a physical analysis of static force, field monitoring, periodical TLS surveys, and an estimation of the volume of storage using GIS. Our study revealed that both partly and fully saturated debris flows are important hydrogeomorphic processes in the initiation zone because of the steep terrain. The predominant type of flow (partly or fully saturated) is affected by the volume of storage as well as rainfall patterns, which control the amount of water in the storage. In addition, small-scale channel gradients (on the order of meters) formed by erosion and deposition during debris flow events reflect the dominant flow type in the flow. Such interactions between flow characteristics and topography could be explained by a simple analysis of static force at the bottom of the sediment mass.

Our study implies that the volume of storage and the rainfall patterns, which control predominant debris flow type classified by the ratio of the depth of the saturated zone, are potential information to improve debris-flow warning system, since the flow characteristics (e.g., sediment concentration, velocity) is different among debris flow types. In addition, our study elucidated that the slope gradient of geomorphic units is the key factor in the estimation of predominant type of the sediment transport processes in the Ohya landslide, where stony debris flows occur due to the mobilization of storage laid on the steep channel. Therefore periodical measurement of the topography in debris flow initiation zones is considered to be essential for the better risk assessment of debris-flow hazards. Because the initiation mechanism of the debris flow and the important force inside of the flow (e.g., frictional force, grain collision) varies affected by the site conditions (e.g., grain size of material, slope gradient), monitoring data in other debris flow torrents are needed for the further understanding of interactions between the debris flow characteristics and the topography.

## Acknowledgement

This study was supported by JSPS Grant Numbers 25702014, 26292077, and 26282076. Airborne DEM was provided by Shizuoka River Office, Chubu Regional Bureau, Ministry of Land, Infrastructure, Transport and Tourism, Japan.

## References

- 5 Arattano, M.: On the use of seismic detectors as monitoring and warning system for debris flows, *Nat. Hazards*, 20, 197–213, 1999.
- Arattano, M., Marchi, L., and Cavalli, M.: Analysis of debris-flow recordings in an instrumented basin: confirmations and new findings, *Nat. Hazards Earth Syst. Sci*, 12, 679–686, 2012.
- Berger, C., McArdell, B. W., and Schlunegger, F.: Sediment transfer patterns at the Illgraben catchment, Switzerland:  
10 Implications for the time scales of debris flow activities, *Geomorphology*, 125, 421–432, 2011a.
- Berger, C., McArdell, B. W., and Schlunegger, F.: Direct measurement of channel erosion by debris flows, Illgraben, Switzerland. *J. Geophys. Res*, 116, F01002, 2011b, doi:10.1029/2010JF001722
- Berti, M., Genevois, R., Simoni, A., and Tecca, P. R.: Field observations of a debris flow event in the Dolomites, *Geomorphology*, 29, 265–274, 1999.
- 15 Bovis M. J., and Jakob, M.: The roll of debris supply conditions in predicting debris flow activity, *Earth Surf. Process. Landf.*, 24, 1039–1054, 1999.
- Carson, M. A.: Angle of repose, angle of shearing resistance and angle of talus slopes, *Earth Surf. Process.*, 2, 368–380, 1977.
- Chen, H. X., Zhang, L. M., Chang, D. S., and Zhang, S.: Mechanisms and runout characteristics of the rainfall triggered debris flow in Xiaojiagou in Sichuan Province, China, *Nat. Hazards*, 62, 1037–1057, 2012.
- 20 Coe J. A., Kinner D. A., Godt J. W.: Initiation conditions for debris flows generated by runoff at Chalk Cliffs, central Colorado, *Geomorphology*, 96, 270–297, 2008.
- Coussot, P., and Meunier, M.: Recognition, classification and mechanical description of debris flows, *Earth-Sci. Rev.*, 40, 209–227, 1996.
- Cui, P., Hu, K., Zhuang, J., Yang, Y., and Zhang, J.: Prediction of debris-flow danger area by combining hydrological and  
25 inundation simulation methods, *J. Moun. Sci.*, 8, 1–9, 2011, doi: 10.1007/s11629-011-2040-8
- Degetto, M., Gregoretto, C., Bernard M.: Comparative analysis of the differences between using LiDAR contour-based DEMs for hydrological modeling of runoff generating debris flows in the Dolomites, *Front. Earth Sci.*, 3, 21, 2015, doi:10.3389/feart.2015.00021
- Dorren, L. K. A.: A review of rockfall mechanics and modelling approaches, *Prog. Phys. Geogr.* 27, 1, 69–87, 2003.
- 30 Drăguț L., and Eisank, C.: Object representations at multiple scales from digital elevation models, *Geomorphology*, 129, 183–189, 2011.

- Egashira, S., Itoh, T. and Takeuchi, H.: Transition mechanism of debris flows over rigid bed to over erodible bed, *Phys. Chem. Earth, Part B: Hydrology, Oceans and Atmosphere*, 26, 169–174, 2001, doi:10.1016/S1464-1909(00)00235-5
- Gabet E. J.: Sediment transport by dry ravel, *J. Geophys. Res.*, 108(B1), 2049, 2003, doi: 10.1029/2001JB001686
- Gregoretti, C.: The initiation of debris flow at high slopes: experimental results, *J. Hydraul. Res.*, 38, 83-88, 2000.
- 5 Gregoretti, C., Dalla Fontana, D.: The triggering of debris flow due to channel-bed failure in some alpine headwater basins of the Dolomites: analyses of critical runoff, *Hydrol. Process.*, 22, 2248–2263, 2008, doi: 10.1002/hyp.6821
- Hayakawa Y., Imaizumi, F., Hotta, N., and Tsunetaka, H.: Towards Long-Lasting Disaster Mitigation Following a Megalandslide: High-Definition Topographic Measurements of Sediment Production by Debris Flows in a Steep Headwater Channel, In *Geomorphology and Society*, Springer, 2016.
- 10 Horn, B. K. P.: Hill shading and the reflectance map, *Proc. IEEE*, 69(1), 14–47, doi:10.1109/PROC.1981.11918, 1981.
- Hu, K., Wei, F., and Li, Y.: Real-time measurement and preliminary analysis of debris-flow impact force at Jiangjia Ravine, China, *Earth Surf. Process. Landf.*, 36, 1268–1278, 2011.
- Hunger, O.: Classification and terminology, In *Debris-flow Hazards and Related Phenomena*, Praxis, Springer, Berlin Heidelberg, 106–134, 2005.
- 15 Hürlimann, M., Abancó, C., Moya, J., and Vilajosana, I.: Results and experiences gathered at the Rebaixader debris-flow monitoring site, Central Pyrenees, Spain, *Landslides*, 11, 939–953, 2014. doi: 10.1007/s10346-013-0452-y
- Hürlimann, M., McArdeell, B. W., and Rickli, C.: Field and laboratory analysis of the runout characteristics of hillslope debris flows in Switzerland, *Geomorphology*, 232, 20–32, 2015. doi:10.1016/j.geomorph.2014.11.030
- Imaizumi, F., Tsuchiya, S., and Ohsaka, O.: Behaviour of debris flows located in a mountainous torrent on the Ohya landslide, 20 *Japan, Can. Geotech. J.*, 42, 919–931, 2005.
- Imaizumi, F., Sidle, R. C., Tsuchiya, S., and Ohsaka, O.: Hydrogeomorphic processes in a steep debris flow initiation zone, *Geophys. Res. Lett.*, 33, L10404, 2006.
- Imaizumi, F., Nishii, R., Murakami, W., and Daimaru, H.: Parallel retreat of rock slopes underlain by alternation of strata, *Geomorphology*, 238, 27–36, 2015.
- 25 Imaizumi, F., Trappman, D., Matsuoka, N., Tsuchiya, S., Ohsaka, O. and Stoffel, M.: Biographical sketch of a giant: deciphering recent debris-flow dynamics from Ohya landslide body (Japanese Alps), *Geomorphology*, 272, 102–114, 2016a, <http://dx.doi.org/10.1016/j.geomorph.2015.11.008>
- Imaizumi, F., Tsuchiya, S., and Ohsaka, O.: Behavior of boulders within a debris flow initiation zone, *Int. J. Erosion Control Eng.*, 9(3), 91-100, 2016b, doi:<http://doi.org/10.13101/ijece.9.91>
- 30 Imaizumi F., Tsuchiya, S., and Ohsaka, O.: Field observations of debris-flow initiation processes on sediment deposits in a previous deep-seated landslide site, *J. Mount. Sci.*, 13, 213–222, 2016c, doi: 10.1007/s11629-015-3345-9
- Jakob, M., Bovis, M., and Oden, M.: The significance of channel recharge rates for estimating debris-flow magnitude and frequency, *Earth Surf. Process. Landf.*, 30, 755–766, 2005.

- Kean, J. W., McCoy, S. W., Tucker, G. E., Staley, D. M., and Coe, J. A.: Runoff-generated debris flows: Observations and modeling of surge initiation, magnitude, and frequency, *J. Geophys. Res.*, 18, 2190–2207, 2013, doi:10.1002/jgrf.20148
- Kirkby, M. J., and Statham, I.: Surface stone movement and scree formation, *J. Geology*, 83, 349–362, 1975.
- Lanzoni, S. Gregoretto, C., Stancanelli, L. M. (2017) Coarse-grained debris flow dynamics on erodible beds, *J. Geophys. Res.*,  
5 printing.
- Lin, P. S., Lin, J. Y., Hung, J. C., and Yang, M. D.: Assessing debris-flow hazard in a watershed in Taiwan, *Eng. Geol.*, 66, 295–313, 2002,doi: 10.1016/S0013-7952(02)00105-9
- March, L., Arattano, M., and Deganutti, A. M.: Ten years of debris-flow monitoring in the Morcardo Torrent (Italian Alps), *Geomorphology*, 46, 1–17, 2002.
- 10 Mangeney, A., Bouchut, F., Thomas, N., Vilotte, J. P., and Bristeau, M. O.: Numerical modeling of self-channeling granular flows and of their levee-channel deposits, *J. Geophys. Res.*, 112, F02017, 2007, doi:10.1029/2006JF000469
- McArdell, B. W., Bartelt, P., and Kowalski, J.: Field observations of basal forces and fluid pore pressure in a debris flow, *Geophys. Res Lett.*, 34, L07406, 2007, doi:10.1029/2006GL029183
- McCoy, S. W., Kean, J. W., Coe, J. A., Staley, D. M., Wasklewicz, T. A., and Tucker, G. E.: Evolution of a natural debris  
15 flow: In situ measurements of flow dynamics, video imagery, and terrestrial laser scanning, *Geology*, 38, 735–738, 2010.
- McCoy, S. W., Kean, J. W., Coe, J. A., Tucker, G. E., Staley, D. M., and Wasklewicz, T. A.: Sediment entrainment by debris flows: In situ measurements from the headwaters of a steep catchment, *J. Geophys. Res.*, 117, F03016, 2012, doi:10.1029/2011JF002278
- McCoy, S.W., Tucker, G. E., Kean, J. W., and Coe, J. A.: Field measurement of basal forces generated by erosive debris flows,  
20 *J. Geophys. Res.*, 118, 589–602, 2013, doi:10.1002/jgrf.20041.
- Obanawa, H., Matsukura, Y.: Cliff retreat and talus development at the caldera wall of Mount St. Helens: Computer simulation using a mathematical model, *Geomorphology*, 97, 697–711, 2008.
- Okano, K., Suwa, H., and Kanno T.: Characterization of debris flows by rainstorm condition at a torrent on the Mount Yakedake volcano, Japan, *Geomorphology*, 136, 88–94, 2012.
- 25 Pareschi, M. T., Santacroce, R., Sulpizio, R., and Zanchetta, G.: Volcaniclastic debris flows in the Clanio Vally (Campania, Italy): insights for the assessment of hazard potential, *Geomorphology*, 43, 219–231, 2002.
- Pirotti, F., and Tarolli, P.: Suitability of LiDAR point density and derived landform curvature maps for channel network extraction, *Hydrol. Process.*, 24, 1187 – 1197, 2010, doi: 10.1002/hyp.7582
- Prancevic, J. P., Lamb, M. P., Fuller, B. M.: Incipient sediment motion across the river to debris-flow transition, *Geology*, 41,  
30 191-194, 2014, doi:10.1130/G34927.1
- Schlunegger, F., Badoux, A., McArdell, B. W., Gwerder, C., Schnydrig, D., Rieke-Zapp, D., and Molnar, P.: Limits of sediment transfer in an alpine debris-flow catchment, Illgraben, Switzerland, *Quat. Sci. Rev.*, 28, 1097–1105, 2009.
- Schmidt, J., and Andrew, R.: Multi-scale landform characterization, *Area*, 37.3, 341–350, 2005.

- Staley, D. N., Wasklewicz, T. A., and Blaszczyński, J. S.: Surficial patterns of debris flow deposition on alluvial fans in Death Valley, CA using airborne laser swath mapping data, *Geomorphology*, 74, 152–163, 2006.
- Staley, D. N., Wasklewicz, T. A., and Kean, J. W.: Characterizing the primary material sources and dominant erosional processes for post-fire debris-flow initiation in a headwater basin using multi-temporal terrestrial laser scanning data, *Geomorphology*, 214, 324–338, 2014, doi: j.geomorph.2014.02.015
- 5 Takahashi, T.: An occurrence mechanism of mud-debris flows, and their characteristics in motion. *Annals, DPRI*, 23B2, 405–435 (in Japanese), 1977.
- Takahashi, T.: Debris flow, IAHR Monograph. A.A. Balkema, Rotterdam, 1991.
- Takahashi, T.: Debris flow: Mechanics, Prediction and Countermeasures. Taylor & Francis, Leiden, 448p, 2007
- 10 Takahashi, T.: Debris flow, CRC Press/Balkema, EH Leiden, Netherlands, 2014.
- Takahashi, T.: and Tsujimoto, H.: A mechanical model for Merapi-type pyroclastic flow, *J. Volcanol. Geotherm. Res.*, 98, 91–115, 2000, doi:10.1016/S0377-0273(99)00193-6
- Tsuchiya, S., and Imaizumi, F.: Large sediment movement caused by the catastrophic Ohya-kuzure landslide, *J. Dis. Sci.*, 3(5), 257–263, 2010.
- 15 VanDine, D. F.: Debris flows and debris torrents in the southern Canadian Cordillera, *Can. Geotech. J.*, 22, 44–62, 1985.
- Whipple K. X., and Dunne, T.: The influence of debris-flow rheology on fan morphology, Owens Valley, California, *Geol. Soc. Am. Bull.*, 104, 887–900, 1992.
- Watanabe, S.: Influence of the mixing ratio of water to sediment on the threshold slope of debris flow: a laboratory experiment, *Trans. Jpn. Geomorph. Union*, 15, 349–369 (in Japanese with English abstract), 1994.
- 20 Yamashita, S., and Miyamoto, K.: Sediment Problems: Strategies for Monitoring, Prediction and Control (Proceedings of the Yokohama Symposium), IAHS Publ. no. 217, 67–74, 1993.
- Zhang, S.: A comprehensive approach to the observation and prevention of debris flows in China, *Nat. Hazards*, 7, 1–23, 1993.
- Zhou, G. G. D., Cui, P., Tang, J. B., Chen, H. Y., Zou, Q., Sun, Q. C.: Experimental study on the triggering mechanisms and kinematic properties of large debris flows in Wenjia Gully, *Eng. Geol.*, 194, 52–61, 2015. doi:10.1016/j.enggeo.2014.10.021